Macromolecular Research

Article

DOI 10.1007/s13233-017-5166-x

www.springer.com/13233 pISSN 1598-5032 eISSN 2092-7673

Hydrophobic Comb-Shaped Polymers Based on PPO with Long Alkyl Side Chains as Novel Anion Exchange Membranes

Haeryang Lim
Tae-Hyun Kim*

Organic Material Synthesis Laboratory, Department of Chemistry, Incheon National University, Incheon 22012, Korea

Received September 28, 2017 / Revised September 30, 2017 / Accepted October 4, 2017

Abstract: Hydrophobic comb quaternary ammonium-functionalized poly(2,6-dimethyl-1,4-phenylene oxide) (AQA-PPOs) having long alkyl side chains were prepared as novel anion exchange membranes. The effects of the relative number of alkyl side chains in the polymer on the conductivity, alkaline stability and other physicochemical properties of the corresponding AQA-PPO membranes were also investigated. The membranes made with more alkyl groups displayed greater conductivity and alkaline stability, and this result was attributed to the increased water uptake of these membranes. The A11QA37-PPO membrane, which had the highest alkyl group content, showed a conductivity as high as 46.0 mS cm^{-1} at 20 °C and 101.9 mS cm^{-1} at 80 °C with an IEC of only 1.92 meq g^{-1}.

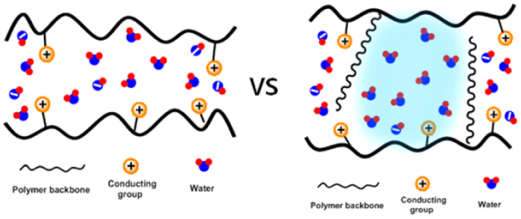

Keywords: anion exchange membranes, hydrophobic comb-shaped polymers, ionic conductivity, alkaline stability, water uptake.

1. Introduction

Anion exchange membrane-based alkaline fuel cells (AEMFCs) have been a topic of increasing interest on account of their various advantages over the better-known and more-developed proton exchange membrane-based fuel cells (PEMFCs). In particular, AEMFCs do not require precious metal-based electrode catalysts, can be constructed using inexpensive metal hardware due to their alkaline operating conditions, exhibit reduced corrosion, and are characterized by fast oxygen reduction kinetics at the cathode.[1-5] The greatest problems arising from the use of anion exchange membranes (AEMs), which are the key component of the AEMFCs, are their relatively low ionic (hydroxide) conductivity and their poor chemical stability under alkaline conditions, especially at elevated temperatures, limiting their practical applications.[6,7] Hence much effort has been devoted to improving the ionic conductivity and chemical (alkaline) stability of the AEMs.[8-11]

Ion conduction in AEMs is largely considered to follow the mechanism proposed by Grotthuss[12] and/or a vehicle mechanism,[13] and water plays an important role as a medium to transport hydroxide ion for both mechanisms. Furthermore, increasing the water content of these membranes facilitates the dissociation of the hydroxide ion from the conducting group, hence facilitating ion conduction.[14] Moreover, recent studies have shown that the chemical stability of the AEMs can also be improved by increasing the amount of water that the membranes take up.[15,16] This improvement was attributed to the water molecules being able to strongly bind the hydroxide, and hence reducing the nucleophilicity of the hydroxide ion by "shielding" it from attacking the conducting group of the AEM.[16] Therefore, increasing the water uptake of the AEM is becoming considered an essential goal for enhancing both its conductivity and alkaline stability.

Increasing the ion-exchange capacity (IEC) of the AEM, with the IEC defined as the number of milliequivalents (meq) of conducting groups per gram of the polymer component of the membrane, has generally been considered to be the easiest way to increase its water uptake and hence conductivity. However, a high IEC is inevitably accompanied by excessive water uptake; this leads to significant swelling and degradation of the physical properties of the membranes.[6,17,18] Therefore, a better approach to enhancing the hydroxide ion conductivity and alkaline stability of the AEM may be to increase the membrane water uptake while maintaining a moderate IEC.

In the current work, we developed a new method to increase the water uptake of AEMs without increasing their IEC values. The method involved introducing a long hydrophobic alkyl (C-12) group and quaternary ammonium groups onto the side chain of the polymer backbone to produce relatively hydrophobic comb-shaped alkyl-substituted and quaternary ammonium-functionalized polymers **5**. We also systematically investigated the effects of the number of alkyl chains per polymer on the conductivity, alkaline stability, and other chemophysical properties of the membranes. The introduction of the alkyl groups was found to increase the water uptake of the polymers, and to increase the hydroxide ion conductivity and alkaline stability of the AEMs. These results were attributed to the introduced alkyl groups acting as a plasticizer to interfere with the interactions between the polymer main chains and to generate additional free volumes, since as described above such free volumes would be expected to promote increased water uptake, and since increased water uptake would be expected to increase

Acknowledgments: This work was supported by the National Research Foundation of Korea (NRF) grant funded by the Korea government (MEST) (NRF-2015M1A2A2058013).

***Corresponding Author:** Tae-Hyun Kim (tkim@inu.ac.kr)

hydroxide ion conductivity and alkaline stability. Note that many similar comb-shaped polymers with long alkyl side chains have been previously developed as AEMs, but most of these research efforts focused on improving the morphology of the membranes by introducing the long alkyl groups on the hydrophilic region, specifically by incorporating both the long alkyl chain and the ion-conducting group (such as ammonium and imidazolium) on the same molecule; and the resulting hydrophilic comb-shaped membranes, while having shown increased conductivity and chemical stability, have also often been found to be brittle, with this brittleness attributed to excessive ionic interactions between the conducting groups.[19-22] To the best of our knowledge, the current work is the first example of introducing a long alkyl side chain on a polymer as a hydrophobic unit with the result of this introduction being an increase in the water uptake levels of the corresponding membranes and the production of relatively hydrophobic comb-shaped AEMs with high levels of conductivity and alkaline stability.

2. Experimental

2.1. Materials

Poly(2,6-dimethyl-1,4-phenylene oxide) (PPO) was obtained from Asahi kasei (M_n: 20.5 kg mol^{-1}, M_w: 49.7 kg mol^{-1}, PDI: 2.42). Zinc chloride ($ZnCl_2$, 98%), lauryl chloride (>98%), trifluoroacetic acid (>99%), and triethylsilane (>98%) were purchased from TCI and chloromethyl methyl ether (CMME, technical grade), aluminum chloride (99.99%), chlorobenzene (99.5%), 1,2-dichloroethane (DCE, anhydrous), and trimethyl amine (TMA, 45 wt% aqueous solution) were purchased from Sigma-Aldrich, *N*-methyl-2-pyrrolidone (NMP, 99%, Daejung chemical), were used as received. All other chemicals, unless otherwise mentioned, were obtained from commercial sources and used as received. Distilled water was used throughout this study.

2.2. Synthesis of the alkyl-substituted and quaternary ammonium-functionalized PPOs (AQA-PPOs) with different alkyl content

2.2.1. Acylation of the PPO 1 to produce the acylated PPO (Ac-PPO, 2) with different acylation degree

A typical procedure to prepare the acylated PPO (Ac-PPO) with different acylation degree (or mol% of acylation) is as follows.

Ac-PPO with degree of acylation of 11 (Ac11-PPO): In a 500 cm^3 two-necked flask equipped with a magnetic stirrer, a nitrogen inlet and a condenser, the poly(2,6-dimethyl-1,4-phenylene oxide) (PPO) (6.0 g, 50 mmol) was completely dissolved in 1,2-dichloroethane (100 cm^3) at 40 °C and cooled to r. t. Aluminum chloride ($AlCl_3$) (0.80 g, 6 mmol) and lauryl chloride (1.31 g, 6 mmol) were then poured into the solution. The resulting mixture was further stirred for 4 h at room temperature. After this time, the resulting solution was treated with methanol (1,000 cm^3), and the resulting precipitated polymer was filtered and washed three times with methanol. The polymer was finally collected and dried at 80 °C under vacuum to give Ac11-PPO as a white fiber (90%); δ_H (400 MHz, $CDCl_3$) 6.50-6.32 (179H, br signal, ArH_2), 6.04-5.96 (11H, br signal ArH_{2a}), 2.95-2.82 (22H, br signal, H_6), 2.24-1.89 (584H, br signal, H_1), 1.75-1.60 (25H, br signal, H_5), 1.40-1.09 (154H, br signal, H_4), 0.90-0.72 (35H, br signal, H_3); (KBr)/cm^{-1} 2922, 2858, 1704, 1596, 1468, 1300, 1180, 1021, 957 and 854.

Ac-PPO with degree of acylation of 7 (Ac7-PPO): Yield of 93%; δ_H (400 MHz, $CDCl_3$) 6.50-6.32 (184H, br signal, ArH_2), 6.04-5.96 (7H, br signal ArH_{2a}), 2.95-2.82 (14H, br signal, H_6), 2.24-1.89 (580H, br signal, H_1), 1.75-1.60 (19H, br signal, H_5), 1.40-1.09 (94H, br signal, H_4), 0.90-0.72 (25H, br signal, H_3).

Ac-PPO with degree of acylation of 3 (Ac3-PPO): Yield of 91%; δ_H (400 MHz, $CDCl_3$) 6.50-6.32 (193H, br signal, ArH_2), 6.04-5.96 (3H, br signal ArH_{2a}), 2.95-2.82 (8H, br signal, H_6), 2.24-1.89 (589H, br signal, H_1), 1.75-1.60 (10H, br signal, H_5), 1.40-1.09 (54H, br signal, H_4), 0.90-0.72 (9H, br signal, H_3).

2.2.2. Reduction of the acylated PPO (Ac-PPO, 2) to produce the alkylated PPO (A-PPO, 3) with different alkyl content

A typical procedure to prepare the alkylated PPO (A-PPO) with different alkyl content is as follows.

A-PPO with alkyl composition of 11 (A11-PPO): Ac11-PPO (5 g, 3.57 mmol) was dissolved in 200 cm^3 of 1,2-dichloroethane (DCE). Subsequently trifluoroacetic acid (TFA) (150 cm^3) and triethylsilane (18 cm^3) were added, and the reaction was heated under stirring to 100 °C for 24 h. After this time, the reaction mixture was poured into 1 M KOH solution until neutral pH was achieved, and this was further poured into 1,000 cm^3 methanol. The polymer was filtered and washed with methanol three times. The polymer was collected as a white powder and dried at 80 °C under vacuum for at least 24 h to give the A-PPO with a yield of 82%; δ_H (400 MHz, $CDCl_3$) 6.55-6.37 (181H, br signal, ArH_2), 6.03-5.96 (10H, br signal, ArH_{2b}), 2.86-2.73 (20H, br signal, H_7), 2.27-1.87 (601H, br signal, H_1), 1.68-1.50 (36H, br signal, H_{6a}), 1.48-1.17 (163H, br signal, H_4 and H_{5a}), 0.91-0.78 (38H, br signal, H_3); (KBr)/cm^{-1} 2922, 2849, 1601, 1467, 1296, 1185, 1017, 957 and 854.

A-PPO with alkyl composition of 7 (A7-PPO): Yield of 82%; δ_H (400 MHz, $CDCl_3$) 6.55-6.37 (184H, br signal, ArH_2), 6.03-5.96 (7H, br signal, ArH_{2b}), 2.86-2.73 (16H, br signal, H_7), 2.27-1.87 (578H, br signal, H_1), 1.68-1.50 (24H, br signal, H_{6a}), 1.48-1.17 (100H, br signal, H_4 and H_{5a}), 0.91-0.78 (21H, br signal, H_3).

A-PPO with alkyl composition of 3 (A3-PPO): Yield of 82%; δ_H (400 MHz, $CDCl_3$) 6.55-6.37 (195H, br signal, ArH_2), 6.03-5.96 (3H, br signal, ArH_{2b}), 2.86-2.73 (7H, br signal, H_7), 2.27-1.87 (595H, br signal, H_1), 1.68-1.50 (23H, br signal, H_{6a}), 1.48-1.17 (44H, br signal, H_4 and H_{5a}), 0.91-0.78 (19H, br signal, H_3).

2.2.3. Chloromethylation of the alkylated PPO (A-PPO, 3) to produce the alkyl-substituted and chloromethylayed PPO (ACl-PPO, 4) with different alkyl content

A typical procedure to prepare the alkylated and chloromethylated PPO (ACl-PPO) with different alkyl content is as follows.

ACl-PPO with alkyl composition of 11 and chloromethylation degree of 37 (A11Cl37-PPO): A11-PPO (3 g, 2.16 mmol) was dissolved in 45 cm^3 of chlorobenzene. Subsequently zinc chloride (150 mg, 5 wt%) and chloromethyl methyl ether (CMME, 2.26 g) were added. The mixture was stirred for 3 h at 50 °C.

After this time, the reaction mixture was poured into methanol (500 cm^3). The polymer was filtered and washed with methanol three times. The polymer was collected as a white fiber and dried at 80 °C under vacuum for at least 24 h to give the A11-Cl37-PPO with a yield of 96% and chloromethylation degree of 37%; δ_H (400 MHz, $CDCl_3$) 6.67-6.37 (105H, br signal, ArH_2), 6.14-5.92 (48H, br signal, ArH_{2c}), 5.06-4.79 (64H, br signal, H_8), 2.99-2.68 (28H, br signal, H_7), 2.47-1.85 (522H, br signal, H_1), 1.67-1.48 (31H, br signal, H_{6a}), 1.48-1.15 (139H, br signal, H_4 and H_{5a}), 0.92-0.77 (26H, br signal, H_3); (KBr)/cm^{-1} 2926, 2853, 1605, 1468, 1309, 1262, 1185, 1017, 957, 854, 716 and 644; GPC ($CHCl_3$, RI)/ Da M_n 3.2×10^4, M_w 12.3×10^4 and M_w/M_n 3.84.

A7Cl37-PPO: Yield of 96% and chloromethylation degree of 37%; δ_H (400 MHz, $CDCl_3$) 6.67-6.37 (113H, br signal, ArH_2), 6.14-5.92 (44H, br signal, ArH_{2c}), 5.06-4.79 (64H, br signal, H_8), 2.99-2.68 (21H, br signal, H_7), 2.47-1.85 (519H, br signal, H_1), 1.67-1.48 (28H, br signal, H_{6a}), 1.48-1.15 (89H, br signal, H_4 and H_{5a}), 0.92-0.77 (21H, br signal, H_3); GPC ($CHCl_3$, RI)/Da M_n 3.5×10^4, M_w 13.6×10^4 and M_w/M_n 3.90.

A3Cl37-PPO: Yield of 96% and chloromethylation degree of 37%; δ_H (400 MHz, $CDCl_3$) 6.67-6.37 (119H, br signal, ArH_2), 6.14-5.92 (41H, br signal, ArH_{2c}), 5.06-4.79 (65H, br signal, H_8), 2.99-2.68 (9H, br signal, H_7), 2.47-1.85 (523H, br signal, H_1), 1.67-1.48 (17H, br signal, H_{6a}), 1.48-1.15 (30H, br signal, H_4 and H_{5a}), 0.92-0.77 (12H, br signal, H_3); GPC ($CHCl_3$, RI)/Da M_n 3.8×10^4, M_w 15.0×10^4 and M_w/M_n 3.92.

A0Cl37-PPO: Yield of 96% and chloromethylation degree of 37%; δ_H (400 MHz, $CDCl_3$) 6.67-6.37 (123H, br signal, ArH_2), 6.14-5.92 (38H, br signal, ArH_c), 5.06-4.79 (64H, br signal, H_8), 2.47-1.85 (513H, br signal, H_1); GPC ($CHCl_3$, RI)/Da M_n 3.9×10^4, M_w 16.3×10^4 and M_w/M_n 4.20.

2.2.4. Functionalization of the chloromethylated PPO (ACl-PPO, 4) to produce the alkyl-substituted and quaternary ammonium-functionalized PPO (AQA-PPO, 5) with different alkyl content

A typical procedure to prepare the alkylated and quaternary ammonium-functionalized PPO (AQA-PPO) with different alkyl content is as follows.

AQA-PPO with alkyl composition of 11 and quaternary ammonium composition of 37 (A11QA37-PPO): A11Cl37-PPO (3 g, 1.91 mmol) was dissolved in 15 cm^3 of *N*-methyl-2-pyrrolidone (NMP). Trimethyl amine (TMA, 45 wt%) (1.97 g, 15 mmol) was added to form a homogeneous mixture. The mixture was stirred for 48 h at 40 °C, and after this time, the reaction mixture was poured into ethyl acetate (250 cm^3). The polymer was filtered and washed with ethyl acetate three times. The polymer was collected as a white powder and dried at 80 °C under vacuum for at least 24 h to give the A11QA37-PPO with a yield of 91%; δ_H (400 MHz, d_6-DMSO) 6.66-6.38 (12H, br signal, ArH_2), 6.34-6.11 (4H, br signal, Ar$H_{2b,2d}$), 5.04-4.60 (7H, br signal, H_{8a}), 3.31-3.04 (21H, br signal, H_9), 2.38-1.75 (50H, br signal, $H_{1,7}$), 1.66-1.45 (3H, br signal, H_{6a}), 1.40-1.08 (15H, br signal, H_4 and H_{5a}), 0.85-0.69 (3H, br signal, H_3).

A7QA37-PPO: Yield of 91%; δ_H (400 MHz, d_6-DMSO), 6.66-6.38 (114H, br signal, ArH_2), 6.34-6.11 (43H, br signal, Ar$H_{2b,2d}$), 5.04-4.60 (74H, br signal, H_{8a}), 3.31-3.04 (229H, br signal, H_9), 2.38-1.75 (501H, br signal, $H_{1,7}$), 1.66-1.45 (27H, br signal, H_{6a}), 1.40-1.08 (93H, br signal, H_4 and H_{5a}), 0.85-0.69 (21H, br signal, H_3).

C3Y37PPO-QA: Yield of 91%; δ_H (400 MHz, d_6-DMSO), 6.66-6.38 (131H, br signal, ArH_2), 6.34-6.11 (35H, br signal, Ar$H_{2b,2d}$), 5.04-4.60 (71H, br signal, H_{8a}), 3.31-3.04 (201H, br signal, H_9), 2.38-1.75 (553H, br signal, $H_{1,7}$), 1.66-1.45 (15H, br signal, H_{6a}), 1.40-1.08 (29H, br signal, H_4 and H_{5a}), 0.85-0.69 (10H, br signal, H_3).

C0Y37PPO-QA: Yield of 91%; δ_H (400 MHz, d_6-DMSO), 6.66-6.38 (123H, br signal, ArH_2), 6.34-6.11 (39H, br signal, ArH_{2d}), 5.04-4.60 (78H, br signal, H_{8a}), 3.31-3.04 (20H, br signal, H_9), 2.38-1.75 (511H, br signal, H_1).

2.3. Fabrication of membranes

All alkyl-substituted and quaternary ammonium-functionalized PPO (AQA-PPO) polymers (0.45 g) in their bromine forms were dissolved in NMP to make their concentrations of 5 wt%. Each solution was then filtered through a cotton plug and poured onto a glass petri dish with an 11 cm diameter. This process resulted in the formation of membranes, which while still on the petri dishes were then dried by heating them at 60 °C for 24 h and 80 °C 4 h in a vacuum. The membranes were then peeled off the dishes containing the membranes by immersion in deionized water. The peeled off membranes were then immersed in 1 M KOH solution at r.t. for 24 h in a closed container to obtain the OH^- forms of the membranes, which were then stored in deionized water for at least 24 h at r.t. prior to further analysis.

2.4. Characterization

^{1}H NMR spectra were obtained on an Agilent 400-MR (400 MHz) instrument using d_6-DMSO or $CDCl_3$ as a reference or internal deuterium lock. FT-IR spectra were recorded on a PerkinElmer FT-IR Spectrum Two spectrometer.

Molar masses were determined by Gel Permeation Chromatography (GPC) using two PL Gel 30 cm × 5 μm mixed C columns at 30 °C running in $CHCl_3$ and calibrated against polystyrene (M_n=600-10^6 g/mol) standards using a Knauer refractive index detector.

The X-ray diffraction patterns of the dry membranes were recorded using a Rigaku HR-XRD smartlab diffractometer by employing a scanning rate of 0.1°/min in a 2θ range from 0° to 2° with a Cu-Kα X-ray (λ=1.54 Å). The dried membranes were placed under vacuum at 80 °C for 12 h prior to the measurement. The X-ray diffraction patterns of the dry membranes were recorded using a Rigaku HR-XRD smartlab diffractometer by employing a scanning rate of 0.1° min^{-1} in a 2θ range from 0° to 4° with a Cu-Kα X-ray (λ=1.54 Å). The samples were equilibrated with 50% RH at least 24 h prior to the measurement.

Glass transition temperature (T_g) was measured by differential scanning calorimetry (DSC) on a perkinElmer DSC 4000. Samples were prepared in aluminium pans and measured from 25-250 °C for 3 cycles. The heating and cooling rate was 10 °C per minute. The third heating was used to determine the glass transition temperature (T_g).

Tensile properties were measured on a Shimadzu EZ-TEST E2-L instrument benchtop tensile tester using a crosshead speed

of 1 mm min^{-1} at 25 °C under 50% relative humidity. The membranes have a thickness between 45 and 50 mm. Engineering stress was calculated from the initial cross sectional area of the sample and Young's modulus (E) was determined from the initial slope of the stress–strain curve. The membrane samples were cut into a rectangular shape with 40 mm × 10 mm (total) and 20 mm × 10 mm (test area).

2.4.1. Ion exchange capacity

The ion exchange capacity of membranes in the hydroxide form was measured by the back titration method. The 20 mg of each membrane sample in its hydroxide form was immersed in a 0.01 M HCl standard solution for 48 h in order to fully neutralize OH^- ions in the membrane. The unreacted HCl was titrated by 0.01 M NaOH standard solution with phenolphthalein as an indicator. The measured IEC value was calculated using the following equation:

$$\mathrm{IEC}_{exp}(\mathrm{meq/g}) = \frac{V_{0NaOH}C_{NaOH} - V_{xNaOH}C_{NaOH}}{W_{dry}}$$

where V_{0NaOH} and V_{xNaOH} are the volume of the NaOH consumed in the titration without and with membranes respectively, C_{NaOH} is the mole concentration of the NaOH which are titrated by the standard oxalic acid solution, and W_{dry} is the weight of the dried membranes.

2.4.2. Conductivity

Hydroxide ion conductivity (σ) in plane direction of each membrane (size: 1 cm × 4 cm in liquid water) was obtained using $\sigma = l/RA$ (l: distance between electrodes, A: cross-sectional area of a membrane coupon). Here, ohmic resistance (R) was measured by two-point probe alternating current (ac) impedance spectroscopy using an electrode systems connected with an impedance/gain-phase analyzer (SI-1260) and an electrochemical interface (SI-1287) over the frequency range from 10 to 200 kHz. The conductivity measurements in liquid water were performed at different temperature range from 20 °C to 80 °C. To minimize unwanted carbonate formation, the cell was completely immersed in degassed and deionized water and the impedance spectrum was collected quickly. The conductivity value was obtained by the average of at least 3 trials with same time intervals.

2.4.3. Water uptake and swelling ratio

The water uptake and swelling ratio of the membranes were measured at both 20 °C and 80 °C. After exchanging membranes with their hydroxide forms, the membranes were soaked into distilled water for more than 24 h. After this time, they were wiped with tissue paper, and the weight and thickness of wet membranes were measured immediately. Afterwards, the membranes were then dried under a vacuum oven at 80 °C until a constant weight and thickness was obtained. The water uptake (WU) and swelling ratio (SR) of the membranes were calculated by following equation:

$$\mathrm{WU}_w(\mathrm{wt\%}) = \frac{W_{wet} - W_{dry}}{W_{dry}} \times 100\%$$

$$\mathrm{SR}(\Delta t) = \frac{t_{wet} - t_{dry}}{t_{dry}} \times 100$$

where, W_{wet} and W_{dry} are the weight of wet and dry membranes and t_{wet} and t_{dry} are the thickness of the wet and dry membranes, respectively.

The IEC, water uptake and swelling ratios were all obtained by the average of 3 different measurements.

2.4.4. Density measurement

The densities of the membranes (g cm^{-3}) were determined experimentally using a top-loading electronic Mettler Toledo balance (XP205, Mettler-Toledo, Switzerland) coupled with a density kit based on Archimedes' principle. The samples were weighed in air and in a liquid with a known density, *i.e.*, high-purity heptane (ρ=0.679 g cm^{-3}). The measurement was taken at r.t. by using the buoyancy method and the density was calculated using the equation

$$\rho_{polymer} = \frac{W_0 - W_1}{W_0} \times \rho_{liquid}$$

where W_0 and W_1 are the weights of the membrane in air and heptane, respectively. The heptane sorption of the membranes was not considered due to their extremely low absorption level.

3. Results and discussion

3.1. Synthesis and characterization of hydrophobic comb-shaped alkyl-substituted and quaternary ammonium-functionalized PPOs (AQA-PPOs)

The syntheses of PPOs having attached to their backbones different relative amounts of the alkyl group as hydrophobic side chains (specifically 3, 7, or 11 mol% of the alkyl group relative to PPO), but all having the same relative amount (37%) of the quaternary ammonium group as conducting group side chains, are described in Scheme 1. The use of PPO as the main polymer backbone was due to its commercial availability and high chemical, mechanical and thermal stability levels.[23-25]

First, an acyl group having a C-12 carbon length was introduced onto the side chain of PPO (**1**) by carrying out Friedel-Crafts acylation using PPO and three different numbers of moles of lauryl chloride and aluminum chloride to give the acylated PPOs (acyl-PPOs, **2**) with the three different relative amounts of the acylated substituent (or acylation degree), *i.e.*, 3, 7, and 11 mol%, and denoted as Ac3-PPO, Ac7-PPO, and Ac11-PPO, respectively. The ketone groups of the three acylated PPOs **2** were then quantitatively reduced, using an excess amount of triethyl silane and trifluoroacetic acid, to the corresponding alkylated (dodecylated) PPOs (A-PPO, **3**), denoted as A3-PPO, A7-PPO, and A11-PPO, respectively.[26] Further chloromethylation of the alkylated PPOs using zinc chloride and chloromethyl methyl ether (CMME) gave the alkyl-substituted and chloromethylated PPOs (ACl-PPO, **4**), which were then functionalized to ammonium using trimethyl amine to produce the desired PPOs having the different relative amounts, 3, 7, and 11 mol%, of the alkyl group and the same relative amount, 37 mol%, of quaternary ammonium

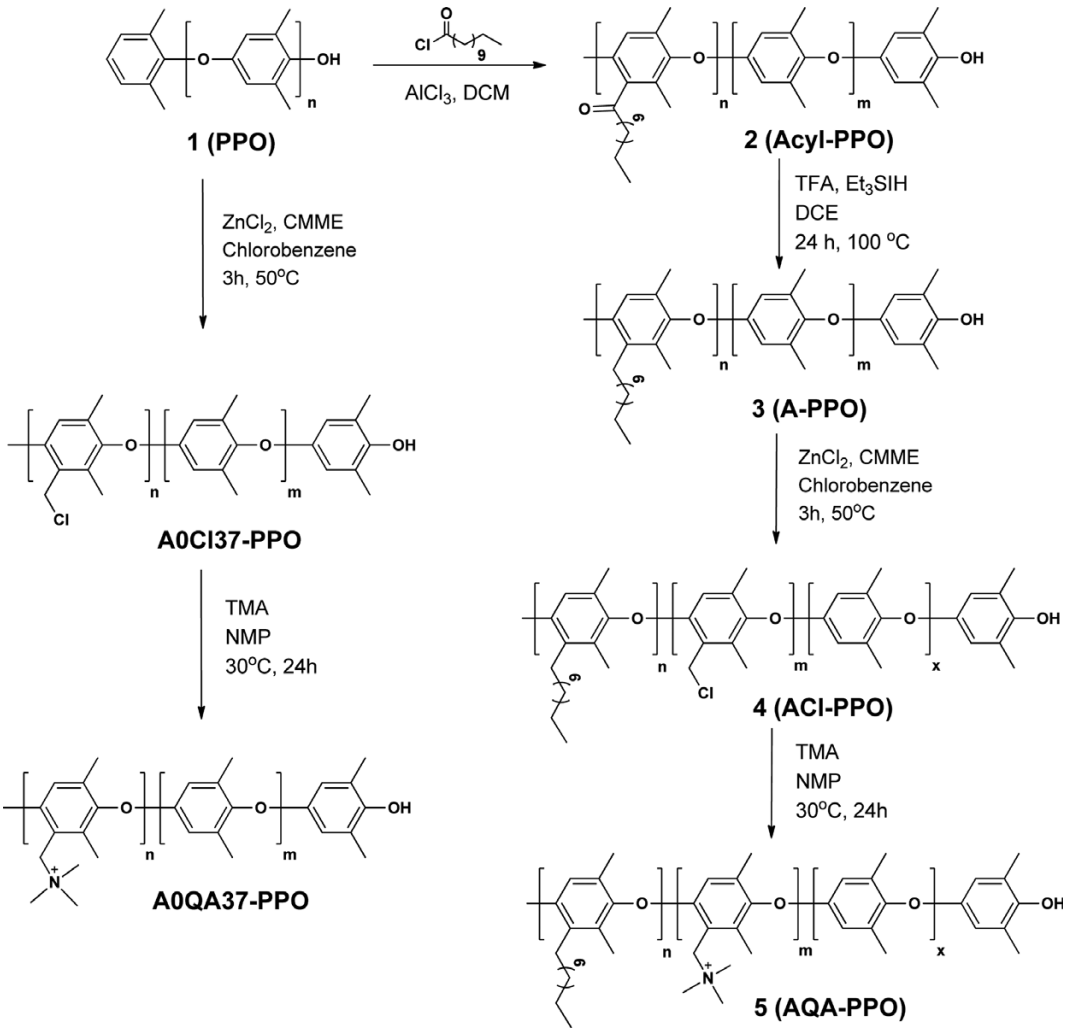

Scheme 1. Synthetic route to the alkyl-substituted and quaternary ammonium-functionalized PPO (AQA-PPO: A3QA37-PPO, A7QA37-PPO, and A11QA37-PPO), and their non-alkylated counterpart (A0QA37-PPO).

group (AQA-PPO, **5**), and denoted as A3QA37-PPO, A7QA37-PPO and A11QA37-PPO, respectively. The PPO with no alkyl substituents but having the same relative amount (37 mol%) of the ammonium group (A0QA37-PPO) was also prepared, by chloromethylating PPO followed by carrying out the ammonium functionalization, to serve as a reference to investigate the effect of the alkyl side chain on the PPO. The chloromethylation was controlled to be 37% and functionalization of the chloromethyl to the ammonium group was found to be almost 100% for all four polymers.

The structural analysis of the PPOs with the four different relative amounts of the alkyl group (0, 3, 7, and 11%) as the hydrophobic unit and the same amount (37%) of the quaternary ammonium as the conducting group was carried out as follows. The acylation was first confirmed by carrying out a comparative ^{1}H NMR spectroscopic analysis: while the spectra of PPO and all three acylation products showed the aromatic peak (H_2) at about 6.46 ppm, the spectra of the products of the acylation reactions showed several peaks not observed in the spectrum of PPO, including an aromatic peak (H_{2a}) at 6.07 ppm with different integrals for the different Ac-PPOs, a characteristic peak of hydrogen (H_6) next to a ketone at 2.94 ppm, and alkyl peaks (H_3, H_4, and H_5) between 0.9 and 1.7 ppm (Figure S1 in Supporting information). The acylation degree for each product was determined by calculating the integral ratio between H_2 (6.46 ppm) and H_{2a} (6.07 ppm), and was found to be 3, 7, and 11%, respectively (Figure S1).

The reduction of the carbonyl groups of the acylated PPOs, **2**, was also confirmed by carrying out ^{1}H NMR spectroscopic analyses. The spectra of the products of the reduction reaction (Figure S2) showed a couple of new peaks not observed in the spectra of the compounds before reduction including an aromatic peak (H_{2b}) at 5.99 ppm and a benzyl peak (H_7) near 2.80 ppm, and did not show the peak at 2.94 ppm, attributed to hydrogen (H_6) next to a ketone, that was observed in the spectra of the compounds before reduction, while all the alkyl protons remained almost the same at the same chemical shifts and with the same relative integrals before and after reduction (Figure S2). The reduction was further confirmed by comparing the IR spectra of the acylated PPOs with those of the reduced forms: the peak corresponding to the C=O vibrational mode of the ketone at 1700 cm^{-1} disappeared after reduction (Figure S3). These observations taken together strongly suggested that the reduction was complete.

Chloromethylation of the alkylated PPO **3** to the alkyl-substituted and chloromethylated PPO (ACl-PPO, **4**) was also confirmed using ^{1}H NMR spectroscopic analysis. The spectra of the products of the chloromethylation reaction (Figure S4), in addition to showing the original aromatic peak H_2 (6.46 ppm), also showed a couple of peaks not observed in the spectra of the compounds just prior to chloromethylation, including an aromatic peak H_{2c} at 6.07 ppm and a broad chloromethyl peak (H_8) at 4.92 ppm. The percent conversion for the chloromethylation reaction was determined by calculating by the integral ratios of the benzyl peak (H_1 at 2.08 ppm in Figure S4) with the new chloromethyl peak (H_8 at 4.92 ppm), and was controlled to be 37% for all four PPOs with the different relative amounts of alkyl groups (A0Cl37-PPO, A3Cl37-PPO, A7Cl37-PPO and A11-Cl37-PPO).

Finally, conversion of ACl-PPO, **4**, to the alkyl-substituted and quaternary ammonium-functionalized PPO (AQA-PPO, **5**) was confirmed by the corresponding disappearance of the chloromethyl peak (H_8 at 4.92 ppm in Figure S4) and appearance of a benzyl peak next to the quaternary ammonium (H_{8a} at 4.78 ppm in Figure S5), together with the appearance of new methyl peaks (H_9 at 3.18 ppm). These results specifically indicated a complete conversion of the chloromethyl group to the quaternary ammonium group.

It should be also mentioned that the molecular weights of the four alkylated and chloromethylated PPOs (ACl-PPOs) were analyzed by GPC, and were found to be almost similar irrespective of the alkyl content (Figure S6 and Table S1). Therefore, the molecular weight effect of our hydrophobic comb-shaped polymers can be ruled out.

3.2. Preparation of the hydrophobic comb-shaped alkyl-substituted and quaternary ammonium-functionalized PPO (AQA-PPO) membranes 5

The alkyl-substituted and quaternary ammonium-functionalized PPO (AQA-PPOs) membranes with the different relative amounts of the alkyl group (0, 3, 7, and 11%) and same relative amount of the quaternary ammonium group (37%) (A0QA37-PPO, A3QA37-PPO, A7QA37-PPO, and A11QA37-PPO) were prepared by casting the NMP solution of the corresponding AQA-PPOs onto a glass plate, followed by vacuum drying. Subsequent immersion of these membranes into a potassium hydroxide solution produced hydrophobic comb-type pendant alkyl-substituted and quaternary ammonium-functionalized PPO (AQA-PPO) membranes with hydroxide counter anions. The obtained AQA-PPOs offered transparent and flexible membranes (Figure 1), and were readily soluble in organic solvents including DMF and DMAc.

3.3. IEC, water uptake and conductivity of the hydrophobic comb-shaped AQA-PPO membranes

The IEC and water uptake are very important factors in determining the ion conductivity and physical properties of AEMs. Theoretical IEC values were calculated using the degree of functionalization determined from the above-described ^{1}H NMR analyses (Table 1). These theoretical IEC values decreased as the alkyl group content was increased. That is, the theoretical IEC value of A0QA37-PPO was greater than that of A3QA37-PPO, which was greater than that of A7QA37-PPO, which in turn was greater than that of A11QA37-PPO. This trend of decreasing IEC, *i.e.*, decreasing number of milliequivalents (meq) of conducting groups per gram of polymer, resulted from the mass of the polymer increasing as the alkyl content was increased while the number of conducting groups was fixed at 37% of the number of polymers. The experimentally determined IEC values, measured by back titration using an NaOH solution, were slightly different from the theoretical IEC values but showed the same tendency, *i.e.*, the IEC decreased as the alkyl content was increased (Table 1).

The water uptake levels of the four membranes, *i.e.*, those having different relative numbers of alkyl groups but the same relative number of ammonium groups, were measured both at 20 °C and 80 °C, and showed greater values at the higher temperature for all four membranes (Table 1). In addition, increased water uptake values were obtained with an increase of the alkyl group content: the water uptake values of A0QA37-PPO, having no alkyl groups, were 33.7% at 20 °C and 62.2% at 80 °C, and these values increased to 42.2% and 74.8% at 20 °C and

Figure 1. Photographs of the hydrophobic comb-shaped alkyl-substituted and quaternary ammonium-functionalized AQA membranes.

Table 1. IEC, water uptake and conductivity values of the alkyl-substituted, quaternary ammonium-functionalized AQA-PPO membranes with different alkyl group contents

Membrane Code	IEC (meq/g)		Water uptake (%)		OH^- conductivity (mS cm^{-1})			
	Theoretical	Experimental	20 °C	80 °C	20 °C	40 °C	60 °C	80 °C
A0QA37-PPO	2.51	2.13	33.7	62.2	37.6	54.9	72.3	84.9
A3QA37-PPO	2.43	2.02	35.2	63.9	39.1	56.2	77.5	87.5
A7QA37-PPO	2.32	1.95	40.0	69.6	44.8	65.1	84.1	94.0
A11QA37-PPO	2.23	1.92	42.2	74.8	46.0	70.1	88.9	101.9

80 °C, respectively, for A11QA37-PPO, which was made with the most alkyl groups. This rather surprising result was ascribed to increased free volumes resulting from the alkyl group side chains interfering with the formation of close-packed interactions between the polymer main chains.

The hydroxide conductivities of all four membranes were measured at temperatures ranging from 20 °C to 80 °C in liquid water. As shown in Figure 2 and Table 1, the conductivity increased with increasing alkyl content: A0QA37-PPO showed conductivity values of 37.6 mS cm^{-1} and 84.9 mS cm^{-1} at 20 °C and 80 °C, respectively, and these values increased to 46.0 mS cm^{-1} and 101.9 mS cm^{-1} for A11QA37-PPO. The conductivity and IEC data for our relatively hydrophobic comb-shaped alkyl-substituted and quaternary ammonium-functionalized PPOs (AQA-PPOs) differed from the typical trend where higher conductivity levels are usually obtained for membranes with higher IEC values. The higher conductivities for our hydrophobic comb-shaped membranes containing more alkyl side chains, despite their lower IEC values, may be related with their increased water uptake, caused by their increased free volume (Table 1).

Ion conductivity is necessarily influenced by the diffusion of ions, and hence increased conductivity is typically obtained at elevated temperatures because ion diffusion is accelerated with an increase of temperature. Likewise, as the water content increases, dissociation of ions from conducting groups is also facilitated. Therefore, as the water content of our AQA-PPO membranes increased, the number of dissociated (hydroxide) ions also increased, and hence increased hydroxide conductivity

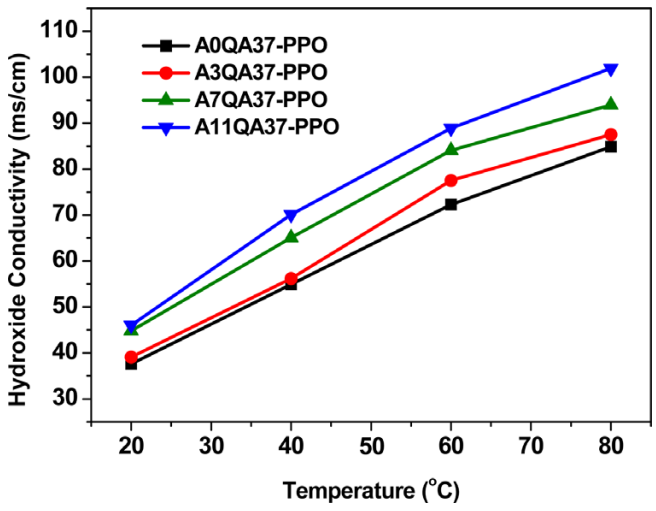

Figure 2. Hydroxide conductivity of the alkyl-substituted and quaternary ammonium-functionalized AQA membranes with different alkyl content as a function of temperature.

was obtained for the membranes having greater water uptake.

3.4. Density and DSC analysis of the hydrophobic comb-shaped AQA-PPO membranes

The densities of the four AQA-PPO membranes were measured in their hydroxide forms, both in dry and fully hydrated states, to investigate the effect of the alkyl group content on the free volume of the membrane (Table 2). A0QA37-PPO, having no alkyl groups, showed the highest density both in the dry state (with a density value of 1.17 g cm^{-3}) and hydrated state (1.12 g cm^{-3}), and these values decreased continuously as the alkyl content was increased (A0QA37-PPO>A3QA37-PPO>A7QA37-PPO>A11QA37-PPO), indicating increased free volumes for the AQA-PPO membranes having more alkyl groups. A11QA37-PPO, having the most alkyl groups, hence showed the lowest density value, both in its dry state (density value of 1.08 g cm^{-3}) and hydrated state (1.03 g cm^{-3}). The densities of all the membranes in their hydrated states were lower than those in their dry states because of low density of water (1.00 g cm^{-3}).

We also set out to determine the glass transition temperature (T_g) values of the four membranes with different alkyl contents using the differential scanning calorimetry (DSC) technique (Figure 3 and Table 2). The highest T_g (214 °C) was obtained for A0QA37-PPO, and the T_g values were found to continuously decrease as the alkyl content was increased. The alkyl groups introduced as side chains of PPO appeared to have acted as a plasticizer, weakening the interactions between the PPO polymer backbones, and hence generating more free volume between the polymer chains, resulting in decreases in both density and T_g values for the AQA-PPO membranes with more alkyl side chains.

Both the density and T_g data were consistent with the water uptake and conductivity data, and they all were attributed to the free volume generated by the introduction of what served as alkyl spacers separating polymer backbones from one another.

Table 2. Density and T_g values of the alkyl-substituted, quaternary ammonium-functionalized AQA-PPO membranes with different alkyl content

Membrane Code	Density (g cm^{-3})		Glass transition temperature (°C)[a]
	Dry	Wet	
A0QA37-PPO	1.17	1.12	214
A3QA37-PPO	1.15	1.11	207
A7QA37-PPO	1.10	1.07	191
A11QA37-PPO	1.08	1.03	174

[a] T_g: Determined from the second heating cycle.

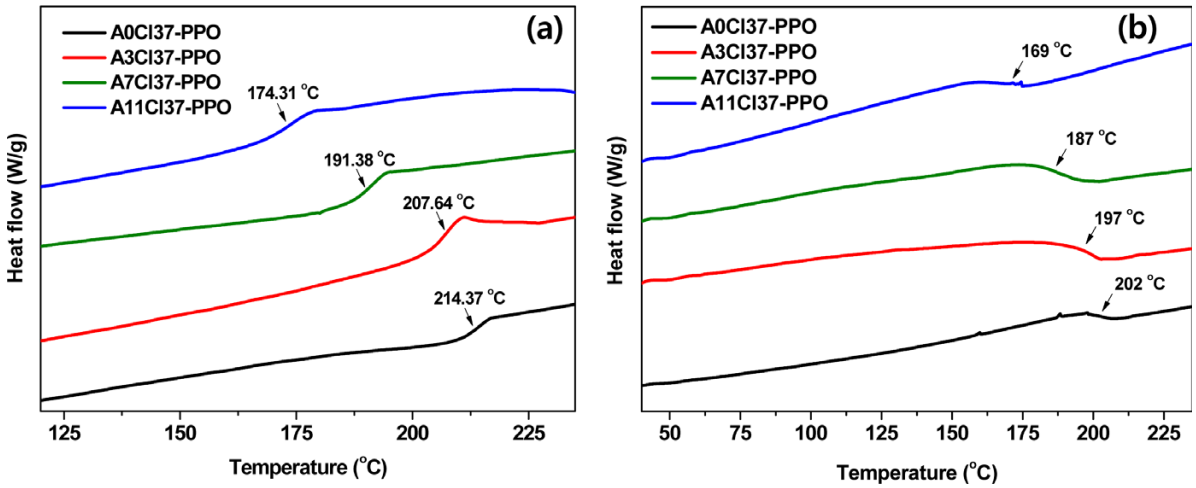

Figure 3. DSC trace for the alkyl-substituted and quaternary ammonium-functionalized AQA membranes with different alkyl content: First cooling cycle (a) and second heating cycle (b) at a rate of 10 °C per minute.

3.5. Morphological analyses of the hydrophobic comb-shaped AQA-PPO membranes

SAXS is an important tool for identifying the morphologies of ionomeric membranes. Ionomeric SAXS peaks were found for all four membranes at a q value of about 0.02 Å, but were slightly shifted toward lower q values as the alkyl content was increased, as shown in Figure 4. This result indicated an increase in the separation lengths (or d-spacings, calculated using the equation $d=2\pi/q$) and was attributed to increasing distances between the ionic domains of the membranes with increasing alkyl content (Table S2). Higher free volumes and hence higher water uptake were, therefore, expected for the membranes having higher alkyl contents, and could also explain the increased conductivity of the AQA-PPO membranes prepared with higher alkyl contents. In fact, the AQA-PPO membrane having the most alkyl groups, *i.e.*, A11QA37-PPO, showed the largest free volume (lowest density) as well as greatest water uptake and conductivity.

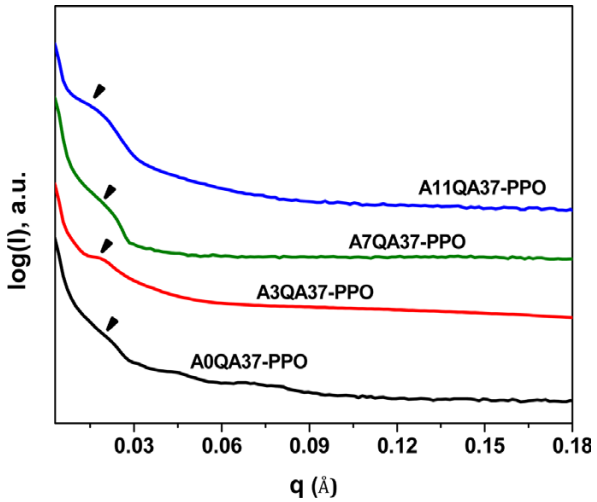

Figure 4. SAXS patterns of the alkyl-substituted and quaternary ammonium-functionalized AQA membranes with different alkyl content.

3.6. Mechanical and dimensional properties of the hydrophobic comb-shaped AQA-PPO membranes

The mechanical properties of the four hydrophobic comb-shaped AQA-PPO membranes having different alkyl contents were assessed at 50% RH. As shown in Figure S7 and Table 3, A0QA37-PPO, having no alkyl groups, showed the highest tensile strength and elongation, and these values generally decreased as the alky group content was increased (except for A7QA37-PPO and A11QA37-PPO, which showed similar tensile strength values), providing further evidence for the plasticization effect of the alkyl side chains. That is, more free volume was generated between the polymer backbones as the alkyl side chains were introduced, resulting in weaker molecular interactions and hence poorer physical properties.

In addition, the swelling ratio of the AQA-PPO membrane was found to increase as its alkyl content was increased, and this result was attributed to enhanced water uptake caused by increased free volume with more alkyl groups (Table 3). Nevertheless, the overall levels of swelling observed for all four AQA-PPO membranes were low, even at a high temperature of 80 °C (Table 3), indicating a relatively high dimensional stability for the alkyl group as a hydrophobic unit and the quaternary ammonium as a conducting group.

Table 3. Mechanical properties and dimensional stability of the AQA-PPO membranes

Membrane Code	Tensile strength (MPa)	Elongation (%)	Young's modulus (GPa)	Swelling ratio (%)	
				20 °C	80 °C
A0QA37-PPO	51.7	99.1	1.19	21.0	28.9
A3QA37-PPO	48.1	82.4	1.15	21.2	29.5
A7QA37-PPO	39.5	55.8	1.08	25.2	35.5
A11QA37-PPO	40.6	46.0	1.05	26.6	36.2

3.7. Alkaline stability of the hydrophobic comb-shaped AQA-PPO membranes

The conducting ion, that is hydroxide, of the AEMs used in the alkaline fuel cell can also function as a nucleophile to decompose not only the polymer backbone but also the ion-conducting group especially at elevated temperature above 80 °C.[27-29] We, therefore, investigated the long-term tolerance levels of our hydrophobic comb-shaped AQA-PPO membranes having alkyl side chains to alkaline conditions by measuring and then comparing their conductivity levels before, during and after immersing them in 1 M KOH at 80 °C for 500 h (Figure 5). The conductivity levels of the four membranes decreased rapidly during the first 100 h and then gradually decreased for the next 400 h. The A0QA37-PPO membrane, in which no alkyl group was introduced, underwent a rapid reduction in conductivity after it was immersed in the 1 M KOH solution at 80 °C: about 60.4% of the initial conductivity of this membrane was lost after it was immersed at 80 °C for only 50 h (Figure 5), and the membrane appeared to be broken into pieces after 250 h at this temperature. In contrast, much less of the initial conductivities of the AQA-PPO membranes containing alkyl side chains were lost in these conditions: for example, only 60.7% of the initial conductivity of the A11QA37-PPO membrane, which was made with the most alkyl groups, was lost after it was immersed in the 1 M KOH solution for 500 h (Figure 5).

These results indicated that the introduction of the alkyl side chains also enhanced the chemical stability of the corresponding membrane. In fact, the three AQA-PPO membranes having the alkyl side chains (A3QA37-PPO, A7QA37-PPO, and A11QA37-PPO) all maintained their original appearance and flexibility even after 500 h in the 1 M KOH solution at 80 °C. As mentioned previously, the water molecules, which strongly bind hydroxide, can reduce the nucleophilicity of the hydroxide by "shielding" it from attacking the conducting group of the AEMs. The increased water uptake levels for the AQA-PPO compounds made with more alkyl side chains were, therefore, thought to have contributed to the enhanced alkaline stability levels of the corresponding membranes.

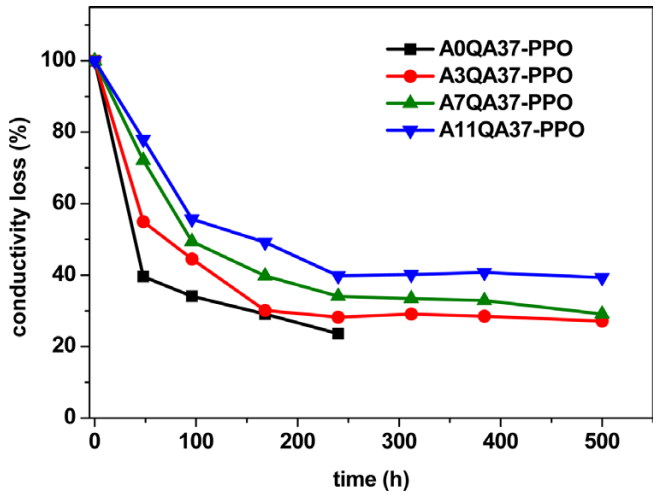

Figure 5. Hydroxide conductivity values of the alkyl-substituted and quaternary ammonium-functionalized AQA membranes with different alkyl contents at various time up to 500 h after alkaline treatment, *i.e.*, with 1 M KOH, at 80 °C (Conductivity was measured at 20 °C).

4. Conclusions

A series of hydrophobic comb-shaped alkyl-substituted and quaternary ammonium-functionalized PPOs (AQA-PPOs) having different numbers of alkyl chains per polymer were prepared as novel anion exchange membranes (AEMs). Unlike other hydrophilic comb-shaped polymers where both the long alkyl chains and conducting groups are incorporated together on the same molecule, our approach was to introduce the long alkyl chain as a hydrophobic unit, separated from the hydrophilic quaternary ammonium-functionalized unit. Our results suggested that the introduced hydrophobic alkyl side chain acted as a plasticizer to interfere with the interaction between the polymer main chains and hence generate more free volumes, thereby increasing the water uptake levels and hence eventually increasing the ion conductivity and alkaline stability levels of the corresponding membranes. We expect that this simple approach we developed will help to tackle the problems arising in AEMs, specifically their relatively low ionic (hydroxide) conductivity and their poor chemical stability under alkaline conditions especially at elevated temperatures, and hence expand the practical applications of AEMFCs.

Supporting information: Information is available regarding the ^{1}H NMR spectra, IR spectra, GPC profiles and stress-strain curves for the samples. The materials are available *via* the Internet at http://www.springer.com/13233.

References

(1) W. Sheng, H. A. Gasteiger, and Y. Shao-Horn, *J. Electrochem. Soc.*, **157**, B1529 (2010).
(2) C. A. Hancock, A. Ong, P. R. Slater, and J. R. Varcoe, *J. Mater. Chem. A*, **2**, 3047 (2014).
(3) J. R. Varcoe, P. Atanassov, D. R. Dekel, A. M. Herring, M. A. Hickner, P. A. Kohl, A. R. Kucernak, W. E. Mustain, K. Nijmeijer, K. Scott, T. Xu, and L. Zhuang, *Energy Environ. Sci.*, **7**, 3135 (2014).
(4) G. Merle, M. Wessling, and K. Nijmeijer, *J. Membr. Sci.*, **377**, 1 (2011).
(5) N. S. Kwak, J. S. Koo, and T. S. Hwang, *Macromol. Res.*, **20**, 205 (2012).
(6) Y. Zha, M. L. Disabb-Miller, Z. D. Johnson, M. A. Hickner, and G. N. Tew, *J. Am. Chem. Soc.*, **134**, 4493 (2012).
(7) O. D. Thomas, K. J. W. Y. Soo, T. J. Peckham, M. P. Kulkarni, and S. Holdcroft, *J. Am. Chem. Soc.*, **134**, 10753 (2012).
(8) E. A. Weiber and P. Jannasch, *ChemSusChem*, **7**, 2621 (2014).
(9) L. Wu, T. Xu, D. Wu, and X. Zheng, *J. Membr. Sci.*, **310**, 577 (2008).
(10) L. Zhu, T. J. Zimudzi, Y. Wang, X. Yu, J. Pan, J. Han, D. I. Kushner, L. Zhuang, and M.A. Hickner, *Macromolecules*, **50**, 2329 (2017).
(11) S. H Kwon, A. H. N. Rao, and T. H. Kim, *J. Power Sources*, doi:10.1016/j.jpowsour.2017.06.047 (2017).
(12) H. Takaba, T. Hisabe, T. shimizu, and Md. K. Alam, *J. Membr. Sci.*, **522**, 237 (2017).
(13) C. Chen, Y. L. S. Tse, G. E. Lindberg, C. Knight, and G. A. Voth, *J. Am. Chem. Soc.*, **138**, 991 (2016).
(14) M. G. Marino, J. P. Melchior, A. Wohlfarth, and K. D. Kreuer, *J. Membr. Sci.*, **464**, 61 (2014).
(15) D. R. Dekel, S. Willdorf, U. Ash, M. Amar, S. Pusara, S. Dhara, S. Srebnik,

and C. E. Diesendruck, *J. Power Sources*, doi:10.1016/j.jpowsour.2017.08.026 (2017).
(16) D. R. Dekel, M. Amar, S. Willdorf, M. Kosa, S. Dhara, and C. E. Diesendruck, *Chem. Mater.*, **29**, 4425 (2017).
(17) Y. J. Kim, C. W. Hwang, S. M. Hyeon, A. Canlier, and T. S. Hwang, *Macromol. Res.*, **25**, 898 (2017).
(18) A. N. Lai, L. S. Wang, C. X. Lin, Y. Z. Zhuo, Q. G. Zhang, A. M. Zhu, and Q. L. Liu, *ACS Appl. Mater. Interfaces*, **7**, 8284 (2015).
(19) N. Li, T. Yan, Z. Li, T. Thurn-Albrecht, and W. H. Binder, *Energy Environ. Sci.*, **5**, 7888 (2012).
(20) J. Pan, C. Chen, Y. Li, L. Wang, L. Tan, G. Li, X. Tang, L. Xiao, J. Lu, and L. Zhuang, *Energy Environ. Sci.*, **7**, 354 (2014).
(21) A. H. N. Rao, S. Nam, and T. H. Kim, *J. Mater. Chem. A*, **3**, 8571 (2015).
(22) H. S. Dang and P. Jannasch, *Macromolecules*, **48**, 5742 (2015).
(23) R. Janarthanan, S. K. Pilli, J. L. Horan, D. A. Gamarra, M. R. Hibbs, and A. M. J. Herring, *Electrochem. Soc.*, **161**, F944 (2014).
(24) A. S. Hay, *J. Polym. Sci., Part A: Polym. Chem.*, **36**, 505 (1998).
(25) A. S. Hay, H. S. Blanchard, G. F. Endres, and J. W Eustance, *J. Am. Chem. Soc.*, **81**, 6335 (1959).
(26) Z. Wang, J. Parrondo, and V. Ramani, *J. Electrochem. Soc.*, **163**, F824 (2016).
(27) M. G. Marino and K. D. Kreuer, *ChemSusChem*, **7**, 1 (2014).
(28) S. Miyanishi and T. Yamaguchi, *Phys. Chem. Chem. Phys.*, **18**, 12009 (2016).
(29) A. D. Mohanty, S. E. Tignor, J. A. Krause, Y. K. Choe, and C. Bae, *Macromolecules*, **49**, 3361 (2016).

